



The 7th International
Conference on Particle Physics
and Astrophysics (ICPPA-2024)



Joint Institute for
Nuclear Research

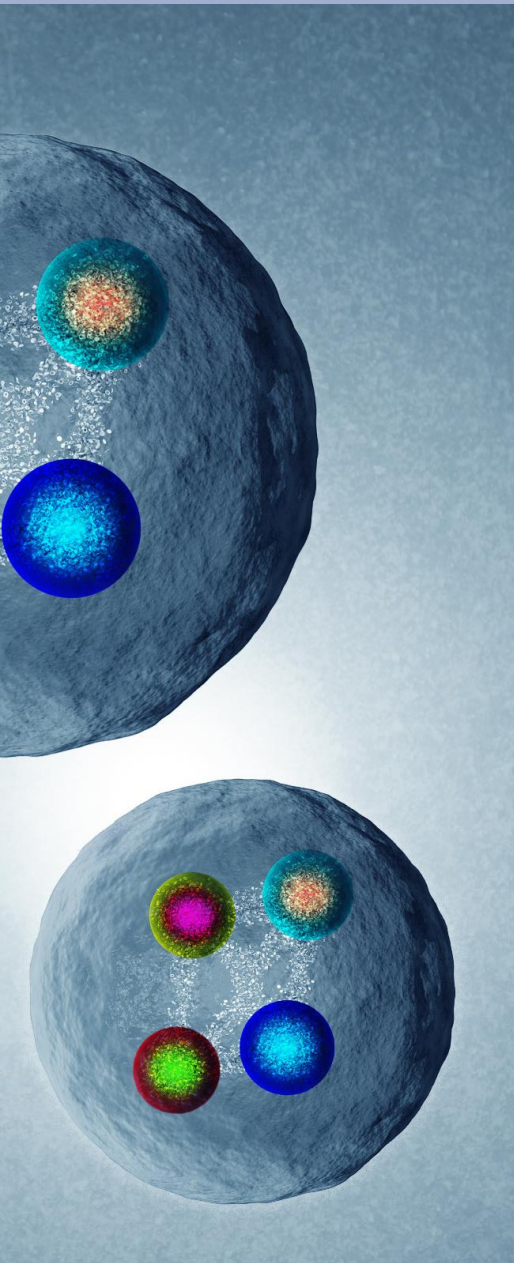


Lomonosov
Moscow State
University

Resonant Charmonium Pair Production: A Comprehensive Review of Theoretical and Experimental Advances

Ivan Yeletsikh, Alisa Didenko

22 – 25 of October 2024



1. Introduction

- motivation and methods of resonance di- J/ψ investigation;
- $T_{cc\bar{c}\bar{c}}$ (X6900 and others) production mechanisms.

2. Experimental observations

- di-charmonium excesses in LHCb, CMS and ATLAS experiments.

3. Predictions of theoretical models

- compact tetraquarks;
- molecule structures.

4. Amplitude analysis of $T_{cc\bar{c}\bar{c}}$

5. Conclusion and outlook

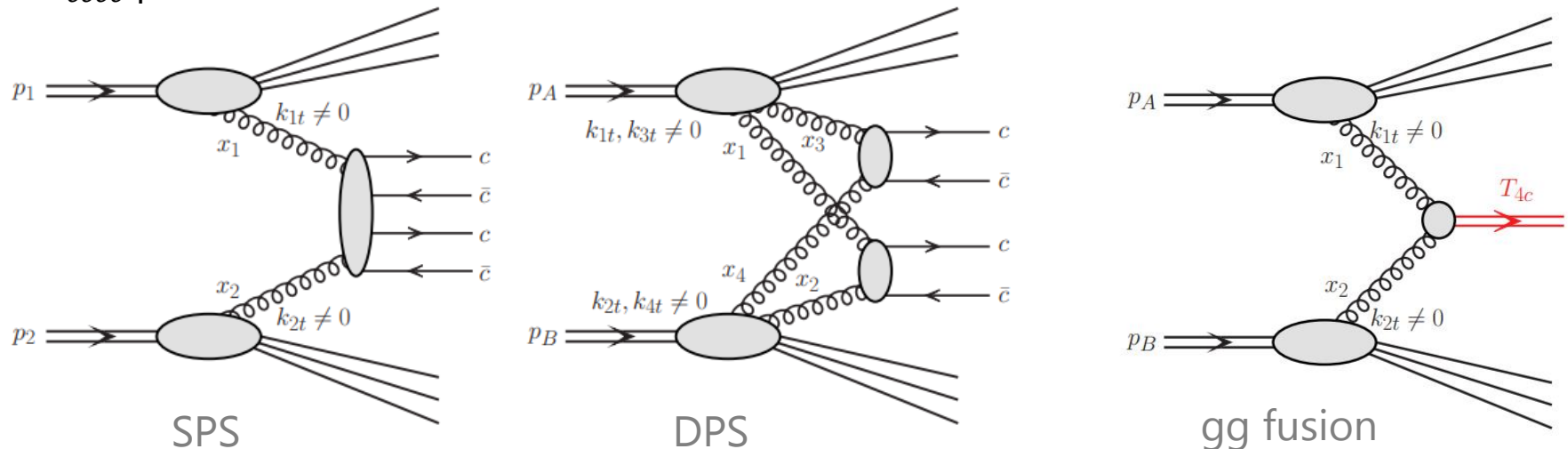
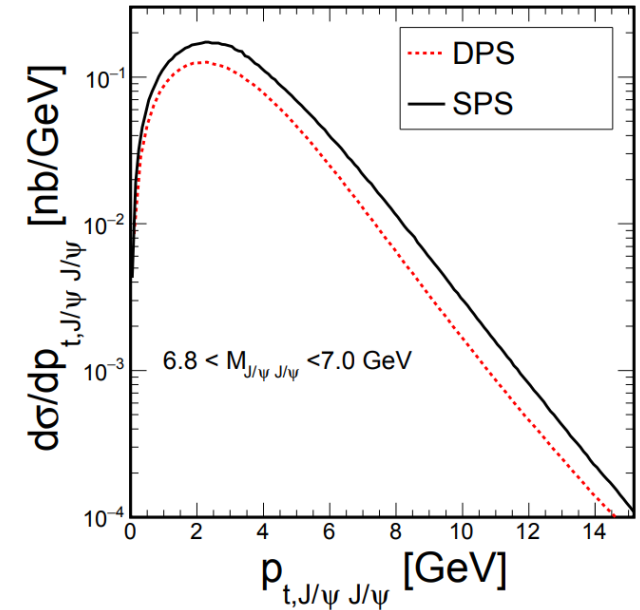
Introduction. $T_{cc\bar{c}\bar{c}}$ production mechanism

The narrow resonant-like structures were discovered by three main LHC collaborations in the di-Jpsi, Jpsi-Psi2S invariant mass spectra suggesting existence of the fully-heavy tetraquarks with a $cc\bar{c}\bar{c}$ configuration.

- 2019-2020: **X(6900)** by LHCb [6]
- 2023: **X(6500), X(6600), X(6900), X(7200)** by ATLAS [7]
- 2024: **X(6500), X(6600), X(6900)** by CMS [8]

[5] On the mechanism of T4c(6900) tetraquark production [arXiv:2009.02100v1]

- Different bound state structures suggest the possibility of different production mechanisms, for example via the DPS mechanism.
- Pt signal spectrum is sensitive to the mechanism of $T_{cc\bar{c}\bar{c}}$ production.

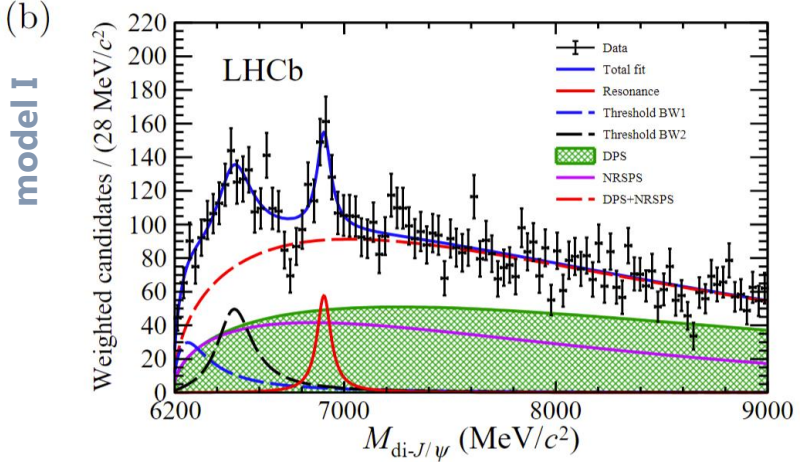
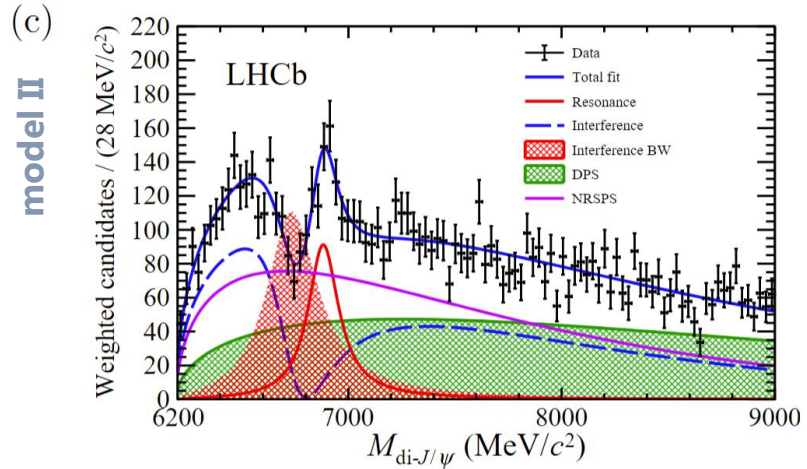
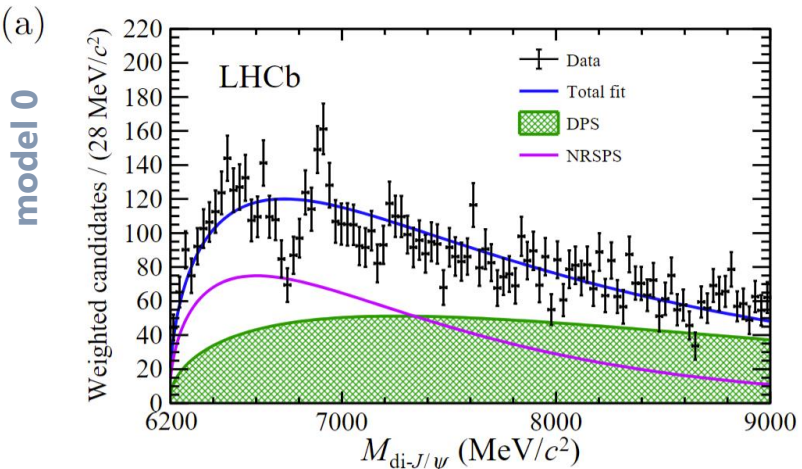


Experimental observation. LHCb

[6] Observation of structure in the J/ψ -pair mass spectrum [\[arXiv:2006.16957v2\]](https://arxiv.org/abs/2006.16957v2)

The discovery of a resonance-like X(6900) signal in the di- J/ψ invariant mass spectrum.

- **Model 0**: non-resonant J/ψ pair production;
- **Model I**: the addition of 3 resonant components;
- **Model II**: interference between the near-threshold structure with the non-resonant SPS and noninterfering resonance at 6900.



X(6900)	No-interference (model I LHCb)	Interference (model II LHCb)
m, GeV	6.905	6.886
Γ, GeV	0.080	0.168

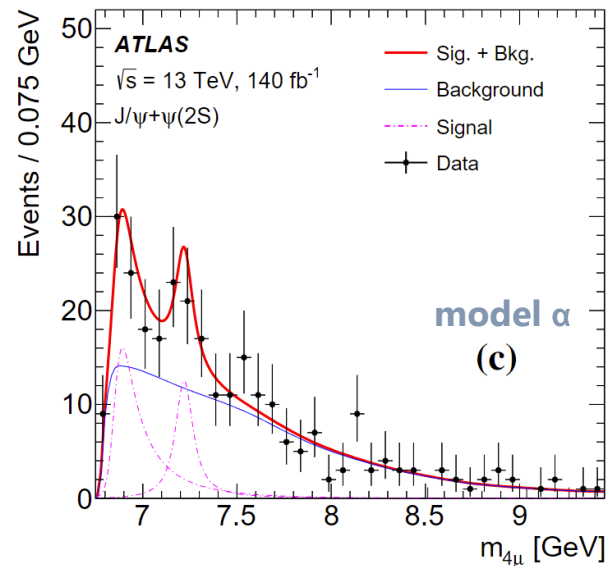
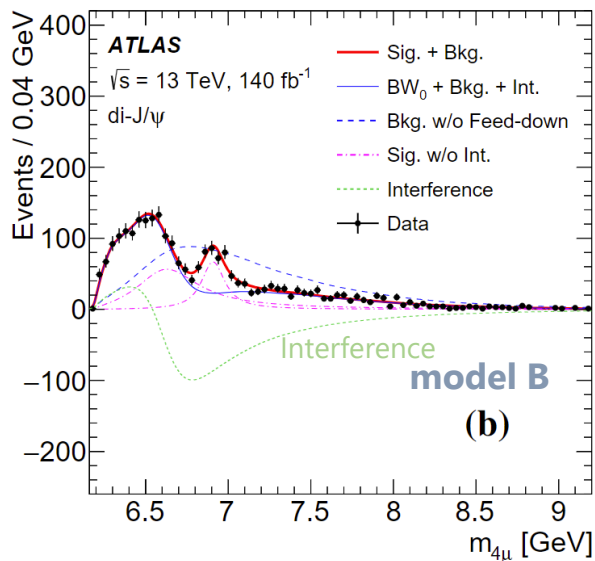
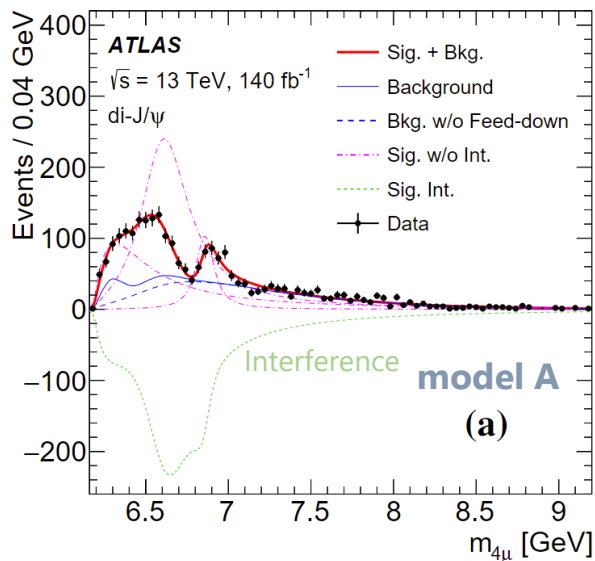
The χ^2 test statistic of the model I corresponding to a probability of 4.6%. The model II has a probability of 15.5%.

Experimental observation. ATLAS

[7] Observation of an excess of di-charmonium events in the four-muon final state with the ATLAS detector [\[arXiv:2304.08962v2\]](https://arxiv.org/abs/2304.08962v2)

- **Model A:** interference of three states with each other;
- **Model B:** threshold structures interferes with SPS, and the second is added without interference;
- **Model α :** mass at 6.9 is fixed on model A, and the state at 7.2 is added without interference.

The mass of the third resonance, m_2 , is consistent with the LHCb mass.



di- J/ψ (ATLAS)

		BW_0	BW_1	BW_2
model A	m, GeV	6.41	6.63	6.86
	Γ, GeV	0.59	0.35	0.11
model B	m, GeV	6.65	-	6.91
	Γ, GeV	0.44	-	0.15

$J/\psi + \psi(2S)$ (ATLAS)

	BW_3
model α	7.22
model β	6.96
	0.51

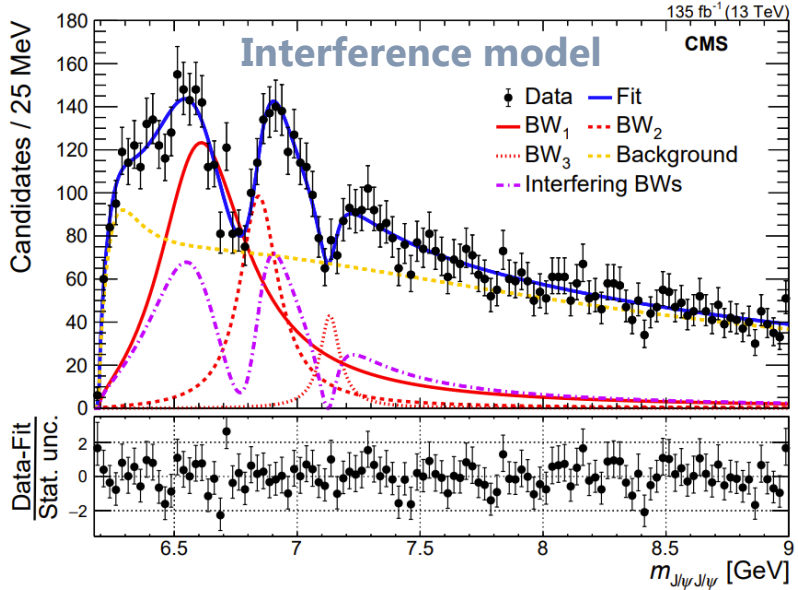
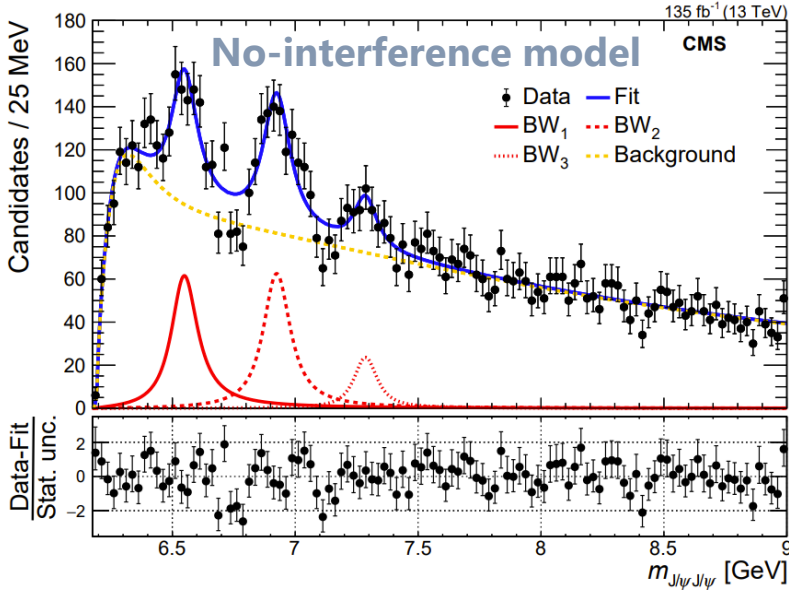
Experimental observation. CMS

[8] New Structures in the $J/\psi J/\psi$ Mass Spectrum in Proton-Proton Collisions at $\sqrt{s} = 13$ TeV [\[arXiv:2306.07164v2\]](https://arxiv.org/abs/2306.07164v2)

Three structures are found in the $J/\psi J/\psi$ invariant mass spectrum by CMS.

- **No-interference model:** the addition of 3 resonant components;
- **Interference model:** interference between 3 resonances.

The model with an interference shows a signal-region χ^2 probability of 65%. The local statistical significances of these 3 peaks are, for increasing mass, 7.9, 9.8, and 4.7 standard deviations.



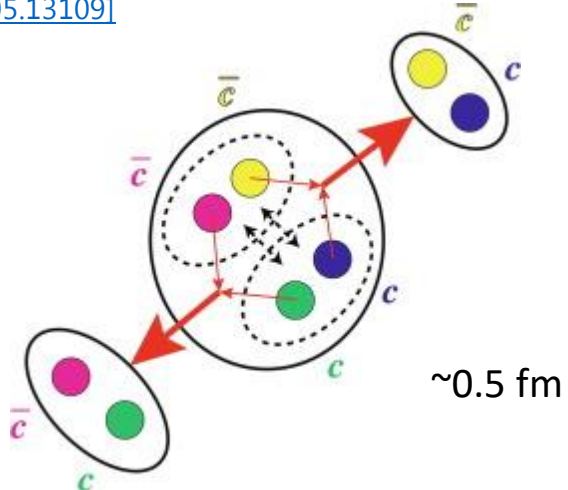
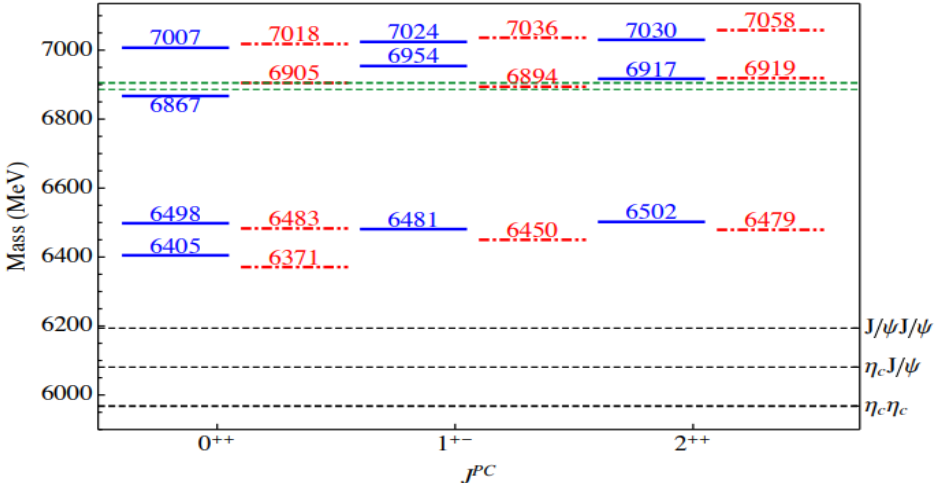
	No-interference (CMS)		
	BW ₁	BW ₂	BW ₃
m, GeV	6.552	6.927	7.287
Γ, GeV	0.124	0.122	0.095

	Interference (CMS)		
	BW ₁	BW ₂	BW ₃
	6.638	6.847	7.134
	0.440	0.191	0.097

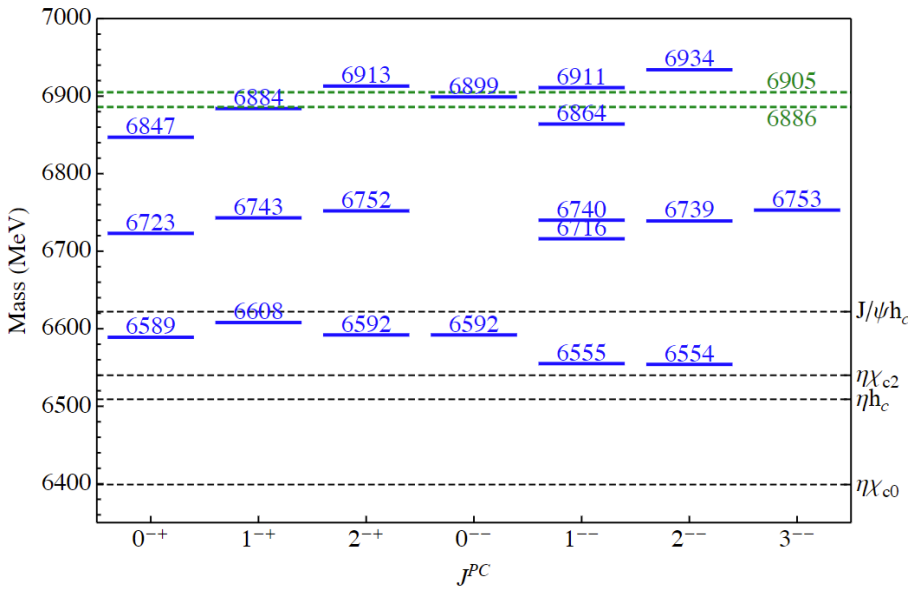
Predictions of theoretical models. Compact tetraquark

Tetraquark models may be composed of the confinement potential plus 'color' interactions

[9] Higher fully-charmed tetraquarks: Radial excitations and P-wave states [\[arXiv:2105.13109\]](https://arxiv.org/abs/2105.13109)



Decay channels:

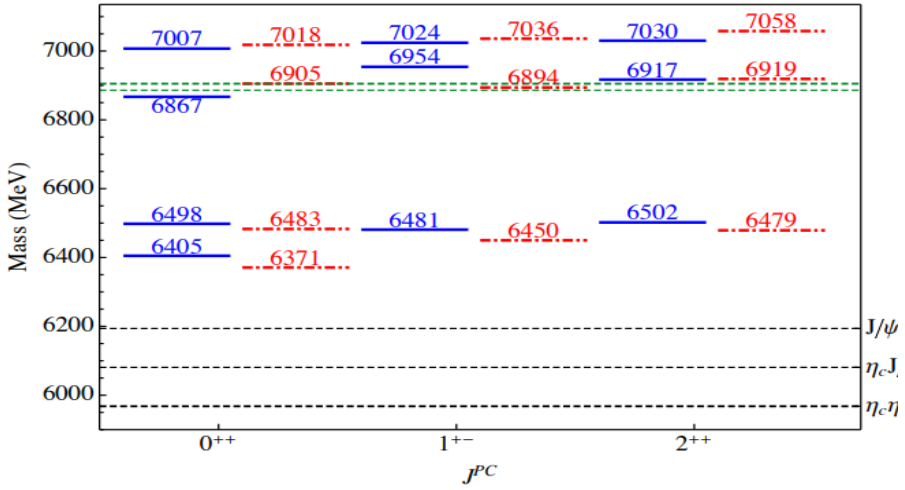


J^{PC}	Decay modes
0^{++}	$\eta_c \eta_c, \mathbf{J}/\psi \mathbf{J}/\psi, \chi_{c1} \eta_c$ (P-wave), $J/\psi h_c$ (1P) (P-wave), $J/\psi \psi$ (2S), $\chi_{c0} \chi_{c0}$
1^{+-}	$\eta_c J/\psi, h_c \eta_c$ (P-wave), $J/\psi \chi_{c1}$ (P-wave), $\eta_c \psi', h_c \chi_{c0}$
2^{++}	$\mathbf{J}/\psi \mathbf{J}/\psi, \eta_c \chi_{c1}$ (P-wave), $\eta_c \chi_{c2}$ (P-wave), $J/\psi h_c$ (P-wave), $J/\psi \psi$ (2S), $\chi_{c0} \chi_{c2}$
0^{-+}	$\mathbf{J}/\psi \mathbf{J}/\psi$ (P-wave), $\eta_c \chi_{c0}, J/\psi h_c, J/\psi \psi$ (2S) (P-wave)
1^{-+}	$\mathbf{J}/\psi \mathbf{J}/\psi$ (P-wave), $J/\psi h_c, J/\psi \psi$ (2S) (P-wave)
2^{-+}	$\mathbf{J}/\psi \mathbf{J}/\psi$ (P-wave), $\eta_c \chi_{c2}, J/\psi h_c, J/\psi \psi$ (2S) (P-wave)
$0^{- -}$	$\eta_c J/\psi$ (P-wave), $J/\psi \chi_{c1}, \eta_c \psi$ (2S) (P-wave)
$1^{- -}$	$\eta_c J/\psi$ (P-wave), $\eta_c h_c, J/\psi \chi_{c0}, J/\psi \chi_{c1}, J/\psi \chi_{c2}, \eta_c \psi'$ (P-wave)
$2^{- -}$	$\eta_c J/\psi$ (P-wave), $J/\psi \chi_{c1}, J/\psi \chi_{c2}, \eta_c \psi'$ (P-wave), $h_c \chi_{c0}$ (P-wave)
$3^{- -}$	$J/\psi \chi_{c2}$

Predictions of theoretical models. Compact tetraquark

Tetraquark models may be composed of the confinement potential plus 'color' interactions

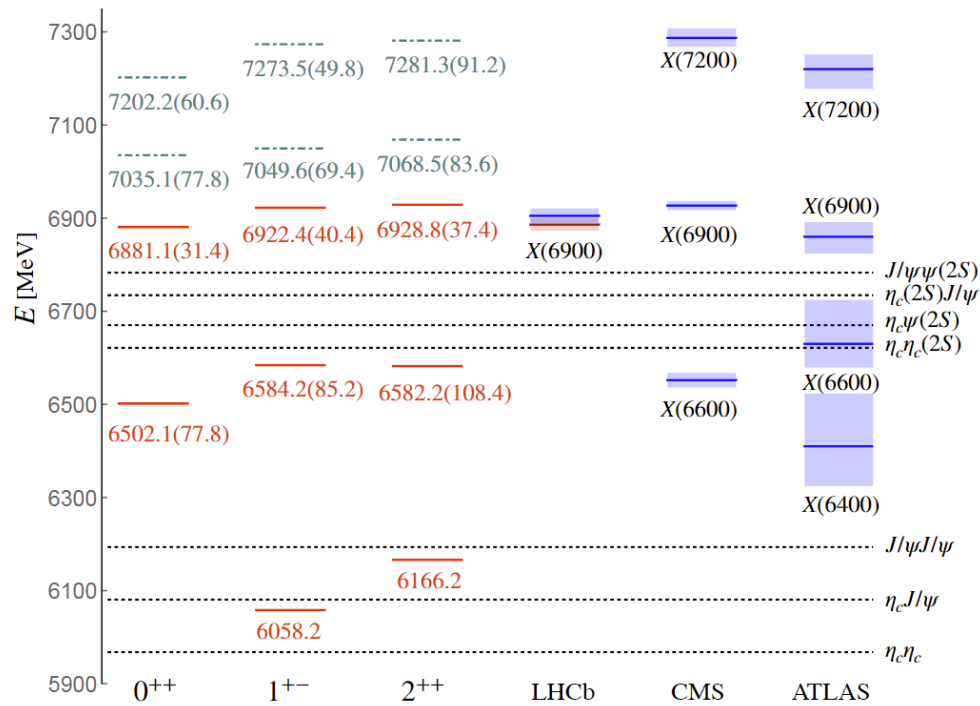
[9] Higher fully-charmed tetraquarks: Radial excitations and P-wave states [\[arXiv:2105.13109\]](https://arxiv.org/abs/2105.13109)



One-gluon-exchange interaction + non-relativistic confinement potential.

- Radial excitations of the S-wave tetraquarks Blue and Red spectra correspond to different model parameters.
- Masses of signals (depending on model parameters) agree with experimental values.
- States at **6405**, **6498**, **6867** and **7007** are predicted for 0^{++}

[10] Quark Confinement for Multi-Quark Systems -- Application to Fully-Charmed Tetraquarks [\[arxiv:2307.04310\]](https://arxiv.org/abs/2307.04310)



A new color basis system and confinement mechanism for multi-quark systems are proposed

- States at **6502**, **6881**, **7035** and **7202** are predicted for 0^{++}
- **Bound states are predicted**

Predictions of theoretical models. Dynamic mechanisms

Compact or molecular structures with **channel rescattering interactions**. Different charmonium pairs directly produced by pp collision may transit into the final state of $J/\psi J/\psi$. [11] Some remarks on $X(6900)$ [\[arxiv:2011.04347\]](https://arxiv.org/abs/2011.04347) *LHCb data

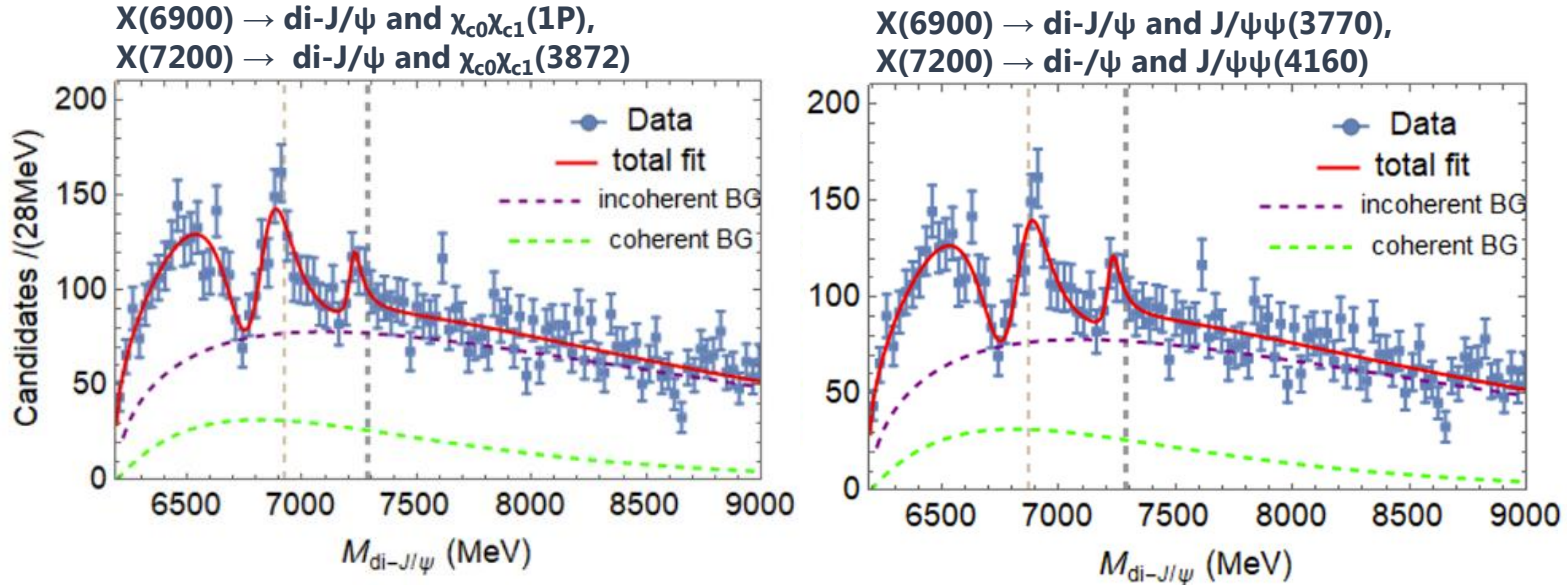


Table I. Involved S -wave couple channels except $di\text{-}J/\psi$.

J^{PC} of $di\text{-}J/\psi$	Couple channels of $X(6900)$	Threshold (MeV)	Couple channels of $X(7200)$	Threshold (MeV)
0^{++}	$J/\psi - \psi(2S)$	6783.0	$J/\psi - \psi(4160)$	7287.9
	$J/\psi - \psi(3770)$	6870.6		
2^{++}	$J/\psi - \psi(2S)$	6783.0	$J/\psi - \psi(4160)$	7287.9
	$J/\psi - \psi(3770)$	6870.6		
	$J/\psi - \psi_2(3823)$	6919.1		
	$J/\psi - \psi_3(3842)$	6939.6		

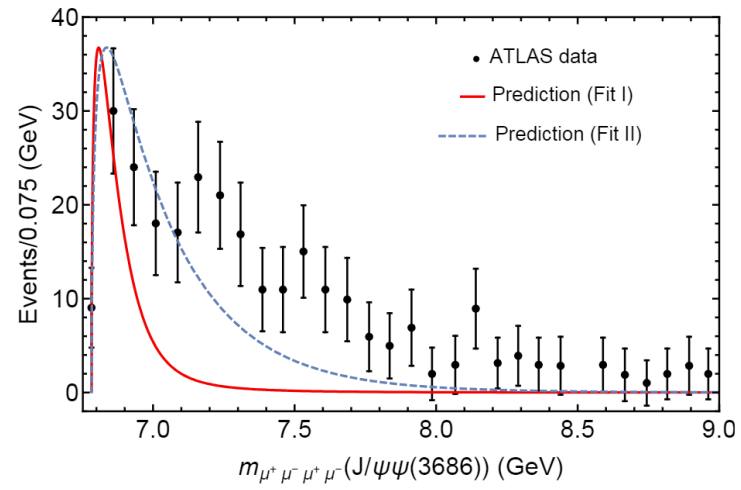
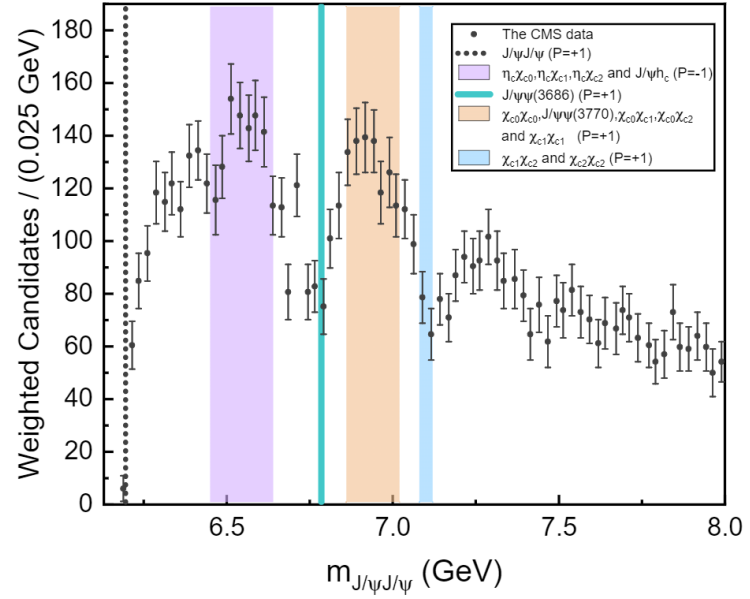
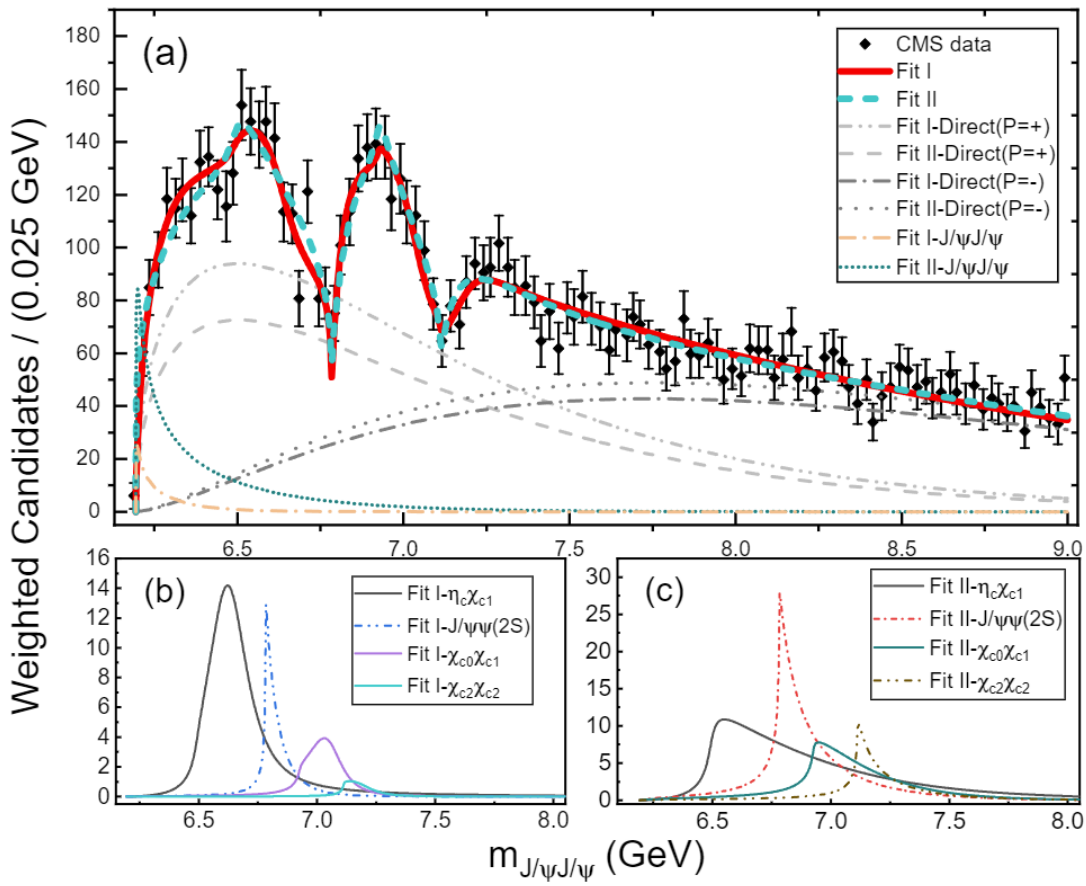
Table II. Involved P -wave couple channels except $di\text{-}J/\psi$.

J^{PC} of $di\text{-}J/\psi$	Couple channels of $X(6900)$	Threshold (MeV)	Couple channels of $X(7200)$	Threshold (MeV)
1^{-+} $(0, 1, 2)^{-+}$	$\chi_{c0} - \chi_{c1}$	6925.4	$\chi_{c0} - \chi_{c1}(3872)$	7286.4
	$J/\psi - \psi(3770)$	6870.6	$J/\psi - \psi(4160)$	7287.9

Predictions of theoretical models. Dynamic mechanisms

[12] Improved understanding of the peaking phenomenon existing in the new di- J/ψ invariant mass spectrum from the CMS Collaboration [[arXiv:2207.04893v3](https://arxiv.org/abs/2207.04893v3)]

The excess di- J/ψ may be due to the transition of different charmonium pairs to the final state J/ψ - J/ψ .



The complete theoretical fit to the invariant mass distribution of J/ψ pair measured by the CMS Collaboration within an extended dynamical mechanism. Four channel interaction included: $\eta_c \chi_{c1}$, $J/\psi \psi(2S)$, $\chi_{c0} \chi_{c1}$, $\chi_{c2} \chi_{c2}$

Predictions of theoretical models. Hadronic molecules

Theories of hadronic molecules are also not excluded

[13] Hadronic $\eta_c \eta_c$, $\chi_{c0} \chi_{c0}$ molecules [\[arXiv:2305.03696\]](#)

The observed signal X(6200) can be interpreted as hadronic scalar molecule $\eta_c \eta_c$, and X(6900) as an another scalar tetraquark molecule of $\chi_{c0} \chi_{c0}$

[14] The X(6900) peak could be a molecular state [\[arXiv:2302.04150\]](#)

The X(6900) peak could be a molecular state of $J/\psi \psi(3770)$ or $\chi_{c0} \chi_c$

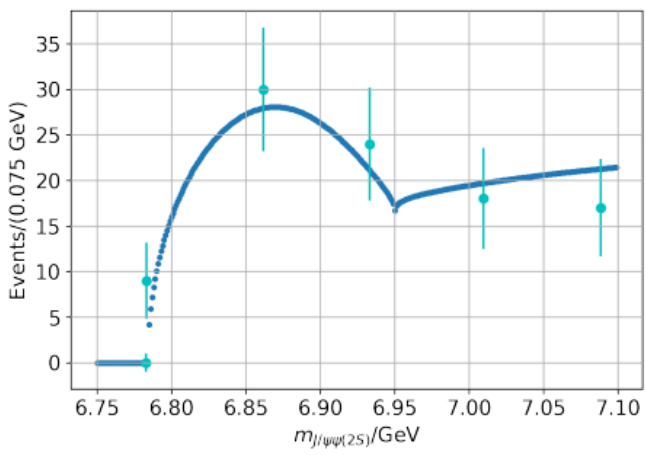
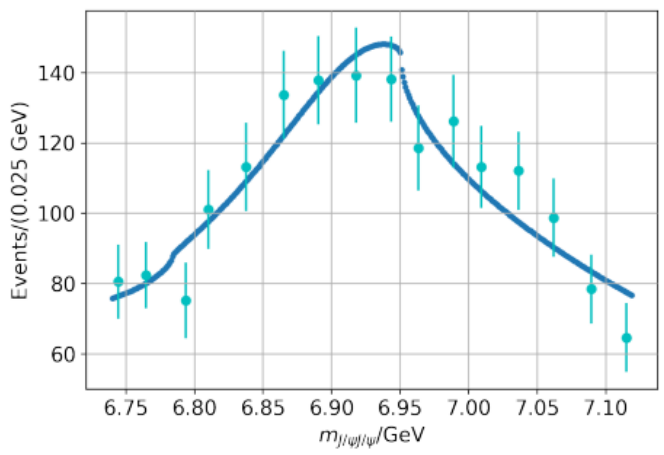


Figure: Fit to the invariant mass spectrum, for the molecule solution.

*The CMS data [\[8a\]](#)

[15] Resonance X(7300): excited 2S tetraquark or hadronic molecule $\chi_{c1} \chi_{c1}$? [\[arXiv:2307.01857v1\]](#)

In accordance to these results, both the excited tetraquark and hadronic molecule may be considered as candidates to the resonance X(7300). Detailed analysis, however, demonstrates that the preferable model for X(7300) is an admixture of the molecule M and sizeable part of X_{4c}^* (first radial excitation X_{4c}^* of the fully charmed diquark-antidiquark state X_{4c})

Amplitude analysis. Decay kinematics of $X_{cc\bar{c}\bar{c}}$ with 4μ in final state

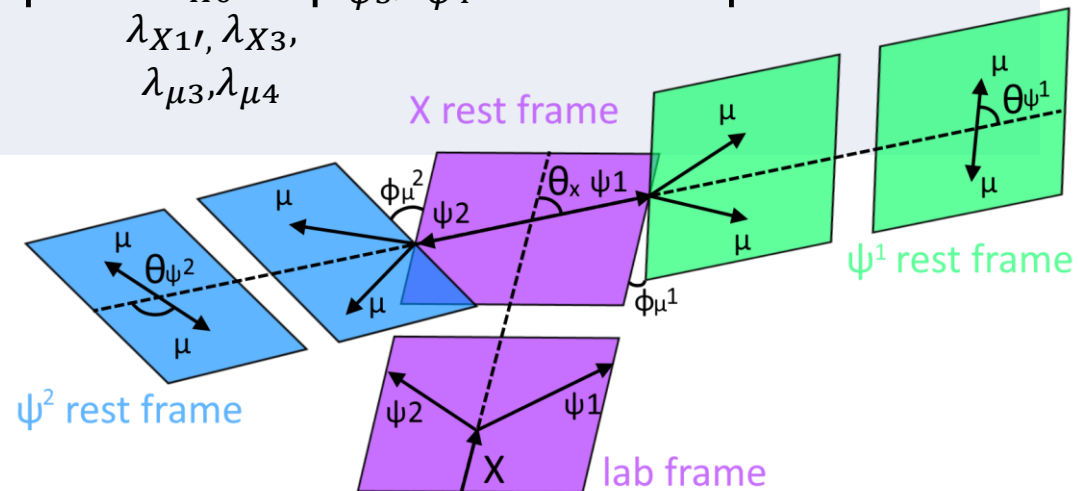
The formalism of helical amplitudes is widely used to describe the angular distributions of decay chains and to obtain the final state in relativistic scattering and decay processes. The amplitudes provide information about the probability of specific decay processes or particle production events.

Helicity formalism:

- Allows for multidimensional fits (invariant mass and angular distributions);
- Gain sensitivity for spin-parity;
- Account interference effects between different amplitudes;
- Takes into account detector effects.

$$M_{total} = \sum_{\substack{\lambda_{X0}, \\ \lambda_{X1}, \lambda_{X2}, \\ \lambda_{\mu1}, \lambda_{\mu2}}} \left| \sum_{\lambda_{\psi1}, \lambda_{\psi2}} A_{di-J/\psi} \right|^2 + \sum_{\substack{\lambda_{X0'}, \\ \lambda_{X1'}, \lambda_{X3}, \\ \lambda_{\mu3}, \lambda_{\mu4}}} \left| \sum_{\lambda_{\psi3}, \lambda_{\psi4}} A_{J/\psi-\psi(2S)} \right|^2$$

- Angular variables determining the kinematics of decay:
 $\theta_X, \phi_{\mu_1}, \theta_{\psi_1}, \phi_{\mu_2}, \theta_{\psi_2}$
- θ_X is the decay angle sensitive to X spin



Conclusion and outlook

- There are many experimental observations of excess mass of $T_{cc\bar{c}\bar{c}}$, but the quantum characteristics have not been researched: LHCb, CMS, ATLAS
- In addition ATLAS analyzed J/psi-psi(2S) channel with 4-muon final states. X6900, X7200 well defined. Low mass threshold effects need investigations in a complex analysis
- There are many theoretical models that describe the spectrum of the invariant mass well. They predict different quantum states
 - Pt signal spectrum is sensitive to the mechanism of $T_{cc\bar{c}\bar{c}}$ production (SPS or DPS)
 - $\text{Cos}(\theta_X)$ is sensitive to J^P of $T_{cc\bar{c}\bar{c}}$
 - Different model predict different decay channels
- We are working on amplitude analysis using the Helicity amplitude formalism of J/ψ meson pairs in the ATLAS data. This can allow to get sensitivity to parameters of exotic states X-6600, X-6900, X-7200

Thank you for your attention

References

- [0] Observation of a narrow charmonium-like state in exclusive $B^+ \rightarrow K^+ \pi^+ \pi^- J/\psi$ decays [\[arXiv:hep-ex/0309032\]](#)
- [1] Observation of a resonance-like structure in the $\pi^+ \pi^- \psi'$ mass distribution in exclusive $B \rightarrow K \pi^+ \pi^- \psi'$ decays [\[arxiv:0708.1790\]](#)
- [2] Observation of X(3872) production in pp collisions at $\sqrt{s} = 7$ TeV [\[arxiv:1112.5310\]](#)
- [3] Observation of the resonant character of the Z(4430)⁻ state [\[arxiv:1404.1903\]](#)
- [4] Observation of J/ψ resonances consistent with pentaquark states in $\Lambda_b^0 \rightarrow J/\psi K^- p$ decays [\[arXiv:1507.03414\]](#)
- [5] On the mechanism of T_{4c}(6900) tetraquark production [\[arXiv:2009.02100v1\]](#)
- [6] Observation of structure in the J/ψ -pair mass spectrum [\[arXiv:2006.16957v2\]](#)
- [7] Observation of an excess of di-charmonium events in the four-muon final state with the ATLAS detector [\[arXiv:2304.08962v2\]](#)
- [8] New Structures in the $J/\psi J/\psi$ Mass Spectrum in Proton-Proton Collisions at $\sqrt{s} = 13$ TeV [\[arXiv:2306.07164v2\]](#)
- [8a] Observation of new structures in the $J/\psi J/\psi$ mass spectrum in pp collisions at $\sqrt{s} = 13$ TeV [\[CMS-PAS-BPH-21-003\]](#)
- [9] Higher fully-charmed tetraquarks: Radial excitations and P-wave states [\[arXiv:2105.13109\]](#)
- [10] Quark Confinement for Multi-Quark Systems -- Application to Fully-Charmed Tetraquarks [\[arxiv:2307.04310\]](#)
- [11] Some remarks on X(6900) [\[arxiv:2011.04347\]](#)
- [12] Improved understanding of the peaking phenomenon existing in the new di- J/ψ invariant mass spectrum from the CMS Collaboration [\[arXiv:2207.04893v3\]](#)
- [13] The observed signals can be interpreted as hadronic $\eta_c \eta_{c'}$ $\chi_{c0} \chi_{c0}$ molecules [\[arXiv:2305.03696\]](#)
- [14] The X(6900) peak could be a molecular state of $J/\psi \psi(3770)$ or $\chi_{c0} \chi_{c2}$ [\[arXiv:2302.04150\]](#)
- [15] Resonance X(7300): excited 2S tetraquark or hadronic molecule $\chi_{c1} \chi_{c1}$? [\[arXiv:2307.01857v1\]](#)

Predictions of theoretical models. Dynamic mechanisms

Compact or molecular structures with **channel rescattering interactions**. [11] Some remarks on X(6900) [[arxiv:2011.04347](https://arxiv.org/abs/2011.04347)] *LHCb data

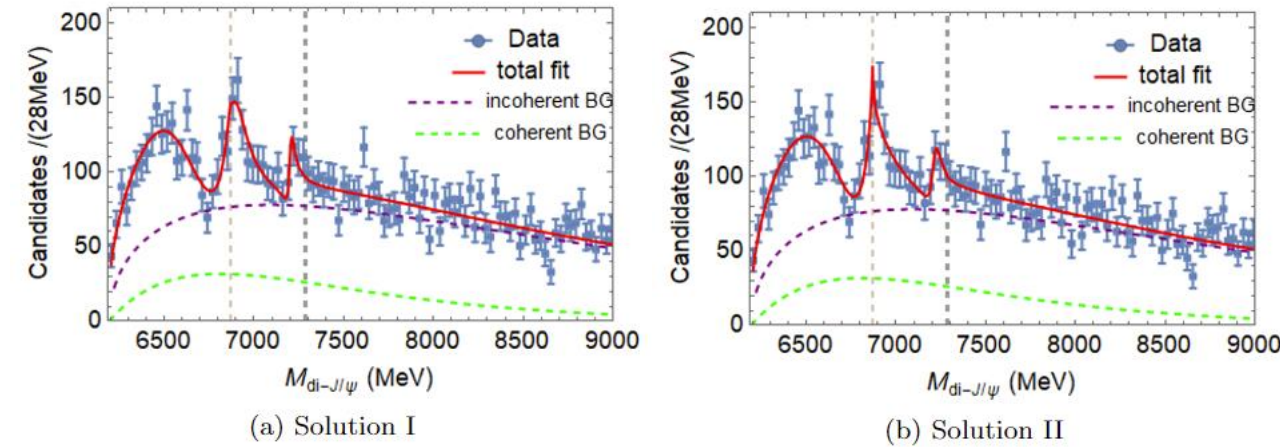


Figure 1.

Fit projections of two solutions for the S-S couplings in Case I with the X(6900) \rightarrow $J/\psi J/\psi$ and $J/\psi\psi(3770)$, and X(7200) \rightarrow $J/\psi J/\psi$ and $J/\psi\psi(4160)$ couples.

The dots with error bars are the LHCb data [6], the red lines are the best fit, the green dashed lines show the coherent BG, the purple dashed lines are the contribution of the incoherent BG, and the vertical lines indicate the corresponding mass thresholds of X(6900) and X(7200).

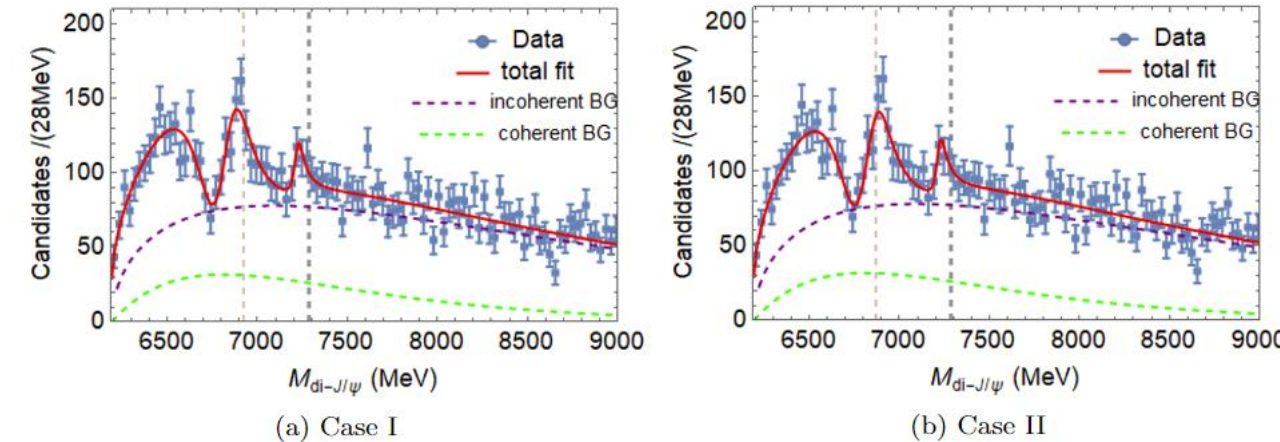


Figure 2.

Fit projections for the P-P couplings, where Fig. (a) shows X(6900) decaying to $J/\psi J/\psi$ and $\chi_{c0}\chi_{c1}$, and X(7200) to $J/\psi J/\psi$ and $\chi_{c0}\chi_{c1}(3872)$, and Fig. (b) illustrates X(6900) \rightarrow $J/\psi J/\psi$ and $J/\psi\psi(3770)$, X(7200) \rightarrow $J/\psi J/\psi$ and $J/\psi\psi(4160)$. Here, the descriptions of the components of the figures are similar to those of Fig. 1.

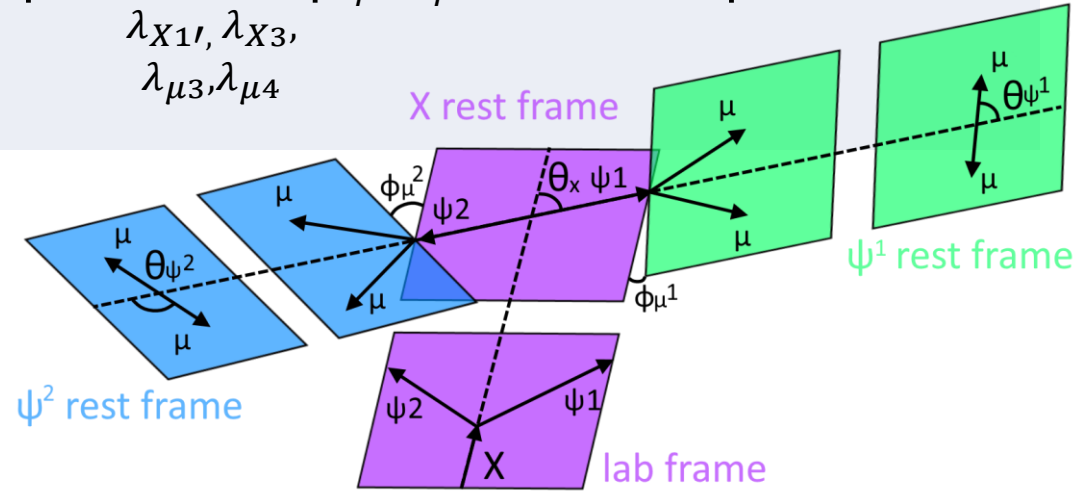
Table III. Parameters for the involved charmonium states [20].

	J/ψ	χ_{c0}	χ_{c1}	$\psi(2S)$	$\psi(3770)$	$\psi_2(3823)$	$\psi_3(3842)$	$\chi_{c1}(3872)$	$\psi(4160)$
J^{PC}	1^{--}	0^{++}	1^{++}	1^{--}	1^{--}	2^{--}	3^{--}	1^{++}	1^{--}
mass (MeV)	3096.9	3414.7	3510.7	3686.1	3773.7	3822.2	3842.7	3871.7	4191.0
$n^{2S+1}L_J$	1^3S_1	1^3P_0	1^3P_1	2^3S_1	1^3D_1	1^3D_2	1^3D_3	2^3P_1 [21]	2^3D_1

Amplitude analysis. Decay kinematics of $X_{cc\bar{c}\bar{c}}$ with 4μ in final state

$$M_{total} = \sum_{\substack{\lambda_{X0}, \\ \lambda_{X1}, \lambda_{X2}, \\ \lambda_{\mu1}, \lambda_{\mu2}}} \left| \sum_{\lambda_{\psi1}, \lambda_{\psi2}} A_{di-J/\psi} \right|^2 + \sum_{\substack{\lambda_{X0'}, \\ \lambda_{X1'}, \lambda_{X3}, \\ \lambda_{\mu3}, \lambda_{\mu4}}} \left| \sum_{\lambda_{\psi3}, \lambda_{\psi4}} A_{J/\psi-\psi(2S)} \right|^2$$

- Angular variables determining the kinematics of decay:
 $\theta_X, \phi_{\mu_1}, \theta_{\psi_1}, \phi_{\mu_2}, \theta_{\psi_2}$
- θ_X is the decay angle sensitive to X spin



$$A = A_{X0} + A_{X1} + A_{X2} + \dots$$

$$A_{Xstate} = A_X * A_{J/\psi_1} * A_{J/\psi_2}$$

$$A_X(\lambda_X, \lambda_{\psi_1}, \lambda_{\psi_2}) = H_{\lambda_\psi, \Delta\lambda_\mu}^{X \rightarrow J/\psi J/\psi} D_{\lambda_X, \lambda_{\psi_1} - \lambda_{\psi_2}}^{J_X}(\phi_\psi, \theta_\psi, 0) * R_X(m_{J/\psi J/\psi}) \quad X \rightarrow J/\psi J/\psi$$

$$A_{J/\psi}(\lambda_\psi, \Delta\lambda_\mu) = D_{\lambda_\psi, \Delta\lambda_\mu}^1(\phi_\psi, \theta_\psi, 0)^* \quad J/\psi_i \rightarrow \mu^+ \mu^-$$

add up coherently

Amplitude analysis. Decay kinematics of $X_{cc\bar{c}\bar{c}}$ with 4μ in final state

$$\mathcal{H}_{\lambda_B, \lambda_C}^{A \rightarrow BC} = \sum_L \sum_S (-1)^{J_B - J_C + L - S + 2\lambda_B - 2\lambda_C} \sqrt{(2L+1)(2S+1)} B_{LS} \times$$

$$\begin{pmatrix} J_B & J_C & S \\ \lambda_B & -\lambda_C & \lambda_C - \lambda_B \end{pmatrix} \begin{pmatrix} L & S & J_A \\ 0 & \lambda_B - \lambda_C & \lambda_C - \lambda_B \end{pmatrix}$$

$$J_\psi = 1,$$

$$P_\psi = -1,$$

$$\vec{S} = \vec{J}_\psi + \vec{J}_\psi = \vec{0}, \vec{1}, \vec{2},$$

$$\vec{P}_X = (P_\psi)(P_\psi)(-1)^L = (-1)(-1)(-1)^L,$$

$$\vec{L} = \vec{J}_X - \vec{S},$$

3j-symbol calculator: <https://www-stone.ch.cam.ac.uk/wigner.shtml>

J_X^P	$H_{\lambda_{\psi_1}, \lambda_{\psi_2}}$	$H_{-\lambda_{\psi_1}, -\lambda_{\psi_2}}$	Явное выражение при заданной спин-четности
0^+	$H_{0,0}$		$-\sqrt{1/3}B_{00} + \sqrt{2/3}B_{22}$
	$H_{0,+1}$	$H_{0,-1}$	0
	$H_{+1,0}$	$H_{-1,0}$	0
	$H_{+1,+1}$	$H_{-1,-1}$	$\sqrt{1/3}B_{00} + \sqrt{1/6}B_{22}$
	$H_{+1,-1}$	$H_{-1,+1}$	0

$$A = A_{X0} + A_{X1} + A_{X2} + \dots$$

$$A_{Xstate} = A_X * A_{J/\psi_1} * A_{J/\psi_2}$$

$$A_X(\lambda_X, \lambda_{\psi_1}, \lambda_{\psi_2}) = H_{\lambda_\psi, \Delta\lambda_\mu}^{X \rightarrow J/\psi J/\psi} D_{\lambda_X, \lambda_{\psi_1} - \lambda_{\psi_2}}^{J_X}(\phi_\psi, \theta_\psi, 0) * R_X(m_{J/\psi J/\psi})$$

add up coherently

$X \rightarrow J/\psi J/\psi$

$$A_{J/\psi}(\lambda_\psi, \Delta\lambda_\mu) = D_{\lambda_\psi, \Delta\lambda_\mu}^1(\phi_\psi, \theta_\psi, 0)^*$$

$J/\psi_i \rightarrow \mu^+ \mu^-$

Amplitude analysis. Decay kinematics of $X_{cc\bar{c}\bar{c}}$ with 4μ in final state

$$R_X(m_{\psi\psi}) = BW(m_{\psi\psi}|M_0^X, \Gamma_0^X) B'_{L_\psi}(q, q_0, d) \left(\frac{q}{M_0^X}\right)^{L_\psi}$$

$$B'_0(p, p_0, d) = 1$$

$$B'_1(p, p_0, d) = \sqrt{\frac{1 + (p_0d)^2}{1 + (pd)^2}}$$

$$BW(m|M_0, \Gamma_0) = \frac{1}{M_0^2 - m^2 - iM_0\Gamma(m)}$$

$$B'_2(p, p_0, d) = \sqrt{\frac{9 + 3(p_0d)^2 + (p_0d)^4}{9 + 3(pd)^2 + (pd)^4}}$$

$$\Gamma(m) = \Gamma_0 \left(\frac{q}{q_0}\right)^{2L_\psi+1} \frac{M_0}{m} B'_{L_\psi}(q, q_0, d)^2$$

$$B'_3(p, p_0, d) = \sqrt{\frac{225 + 45(p_0d)^2 + 6(p_0d)^4 + (p_0d)^6}{225 + 45(pd)^2 + 6(pd)^4 + (pd)^6}}$$

The **Wigner D-matrix** is a unitary square matrix of dimension $2j + 1$ in this spherical basis with elements

$$D_{m'm}^j(\alpha, \beta, \gamma) \equiv \langle jm' | \mathcal{R}(\alpha, \beta, \gamma) | jm \rangle = e^{-im'\alpha} d_{m'm}^j(\beta) e^{-im\gamma}$$

$$d_{m'm}^j(\beta) = [(j+m')!(j-m')!(j+m)!(j-m)!]^{-\frac{1}{2}} \sum_{s=s_{\min}}^{s_{\max}} \left[\frac{(-1)^{m'-m+s} \left(\cos \frac{\beta}{2}\right)^{2j+m-m'-2s} \left(\sin \frac{\beta}{2}\right)^{m'-m+2s}}{(j+m-s)!s!(m'-m+s)!(j-m'-s)!} \right]$$

$$A = A_{X0} + A_{X1} + A_{X2} + \dots$$

add up coherently

$$A_{Xstate} = A_X * A_{J/\psi_1} * A_{J/\psi_2}$$

$$A_X(\lambda_X, \lambda_{\psi_1}, \lambda_{\psi_2}) = H_{\lambda_\psi, \Delta\lambda_\mu}^{X \rightarrow J/\psi J/\psi} D_{\lambda_X, \lambda_{\psi_1} - \lambda_{\psi_2}}^{J_X}(\phi_\psi, \theta_\psi, 0) * R_X(m_{J/\psi J/\psi})$$

$X \rightarrow J/\psi J/\psi$

$$A_{J/\psi}(\lambda_\psi, \Delta\lambda_\mu) = D_{\lambda_\psi, \Delta\lambda_\mu}^1(\phi_\psi, \theta_\psi, 0)^*$$

$J/\psi_i \rightarrow \mu^+ \mu^-$